Paraffin ATR-IR Fingerprints obtained with q-BWF deconvolutions

Paraffin ATR-IR Fingerprints obtained with q-BWF deconvolutions

Amelia Carolina Sparavigna

Department of Applied Science and Technology, Polytechnic University of Turin, Turin, Italy

Abstract: The fingerprint of an ATR-IR spectrum of Paraffin is proposed. The ATR-IR fingerprint is obtained with a q-BWF functions deconvolution, with these functions implemented in Fityk software.

DOI: 10.5281/zenodo.15167750. Torino, 7 April 2025, amelia.sparavigna@polito.it

ATR-IR is a spectroscopic technique using infrared light to analyze the chemical structure of a sample. It allows for the direct examination of solid or liquid samples without the need for further preparation. In ATR, Attenuated Total Reflection, light undergoes multiple internal reflections within a crystal, creating an evanescent wave that penetrates the sample surface, providing valuable molecular information. The evanescent wave interacts with the sample, and the reflected light is then analyzed by the FTIR spectrometer (see the discussion in Sparavigna, 2024, DOI https://dx.doi.org/10.2139/ssrn.4993668). Let us stress that ATR-IR is a surface-sensitive technique, because it primarily analyzes the surface of the sample.

ATR-IR can be used to identify and quantify paraffin in various samples, including beeswax adulteration (Svečnjak et al., 2015, Chatzipanagis et al., 2024). Jamwal and coworkers, 2020, have used ATR-FTIR spectroscopy to detect and quantify paraffin oil in virgin coconut oil adulteration. This swift technique, which requires no redundant sample preparation, and does not use perilous chemicals, can be combined with chemometrics to study food adulteration, besides the cases of beeswax and coconut oil.

Here we propose the ATR-IR 'fingerprint' of paraffin, according to data from the "FTIR spectral library of the major components of archaeological sediments", by Michael Toffolo (Project leader), released under Creative Commons Attribution 4.0 International, available https://zenodo.org/records/14170891. The Zenodo page tells us that "Spectra were collected using a Thermo Scientific Nicolet iS5 spectrometer equipped with an iD1 transmission compartment in the 4000-400 cm^{-1} range at 4 cm^{-1} resolution, and in 32 scans. Spectra were collected with the same instrument and settings in ATR mode using an iD7 ATR diamond crystal compartment. Spectra are available in .spa and .csv formats" (Toffolo, 2024).

Here we use the term "fingerprint" as it was proposed in relation to the Raman spectroscopy. It seems that this term first appeared in an article published in 1947 about the Raman spectra of hydrocarbons by Fenske and coworkers. Fenske et al., 1947, wrote that the "Raman lines, are characteristic of the substance illuminated and are therefore a "fingerprint" of that substance". From that time on, the points of identification, such as positions of peaks, shoulders and valleys create the characteristic spectral pattern which is known as the "Raman fingerprint" of a given material. Of course, if we have the recorded data, we can decompose the spectrum in components, that is, we can perform a 'deconvolution'. Then, the fingerprint can be characterized not only by the positions of the peaks and shoulders, but also by the parameters related to the functions occurring in the deconvolution. In fact, we can have an "extended fingerprint" of the material. For paraffin ATR-IR we propose an extended fingerprint, as we did before, for augelite and albite minerals. The deconvolution of the spectrum is proposed determined by means of asymmetric q-

Gaussian functions, that is the q-BWF functions. These functions (q-Breit-Wigner-Fano functions) have been proposed by Sparavigna in 2023 and represent the generalization in the framework of Tsallis statistics of the Breit-Wigner-Fano functions. Deconvolutions are obtained using Fityk software (Wojdyr, 2010).

q-Gaussian function and its asymmetric q-BWF form

The fitting of Raman spectra with q-Gaussian line shapes has been proposed for the first time https://www.ijsciences.com/pub/article/2671 by A. C. Sparavigna. The q-Gaussian line shape is a function based on the Tsallis q-form of the exponential function (Tsallis, 1988). This exponential form is characterized by a q-parameter. When q is equal to 2, we have the Lorentzian function. If q is close to 1, we have a Gaussian function. For values of q between 1 and 2, we have a bell-shaped symmetric function with power-law wings ranging from Gaussian to Lorentzian tails.

The q-Gaussian is given as $f(x) = Ce_q(-\gamma x^2)$, where $e_q(.)$ is the q-exponential function and C a scale constant (Hanel et al., 2009). The q-exponential has expression: $e_q(u) = [1 + (1-q)u]^{1/(1-q)}$. For spectroscopy, we write the q-Gaussian function with the center of the band at x_o:

$$q\text{-}Gaussian = Cexp_q(-\gamma(x-x_o)^2) = C\,[1 + (q-1)\gamma(x-x_o)^2]^{1/(1-q)}.$$

We can apply q-Gaussian functions by means of Fityk software. In Fityk, a q-Gaussian function can be defined in the following manner:

```
define Qgau(height, center, hwhm, q=1.5) = height*(1+(q-1)*((x-center)/hwhm)^2)^(1/(1-q))
```

where q=1.5 is the initial guessed value of the q-parameter. Parameter hwhm is the half width at half maximum of the line, in the case of a Lorentzian function. In fact, when q=2, the q-Gaussian turns into a Lorentzian function, that we can find defined in Fityk as:

```
Lorentzian(height, center, hwhm) = height/(1+((x-center)/hwhm)^2)
```

When q is close to 1, the q-Gaussian becomes a Gaussian function.

In Fityk, to define a function, use please Session > New Script > Blank Fityk Script

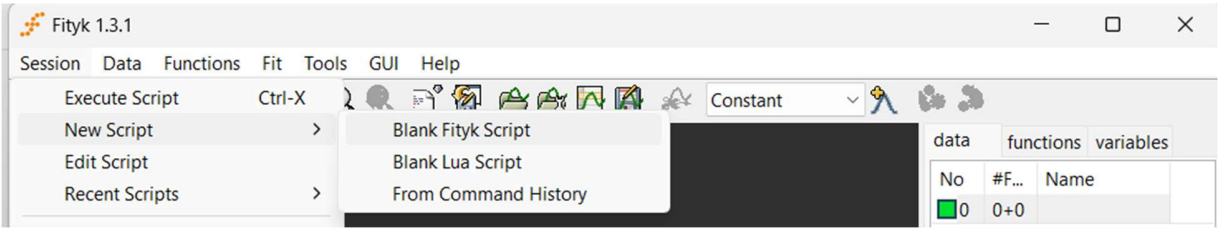

In the Blank Fityk Script paste the "define" of the function, for instance the Qgau given above.

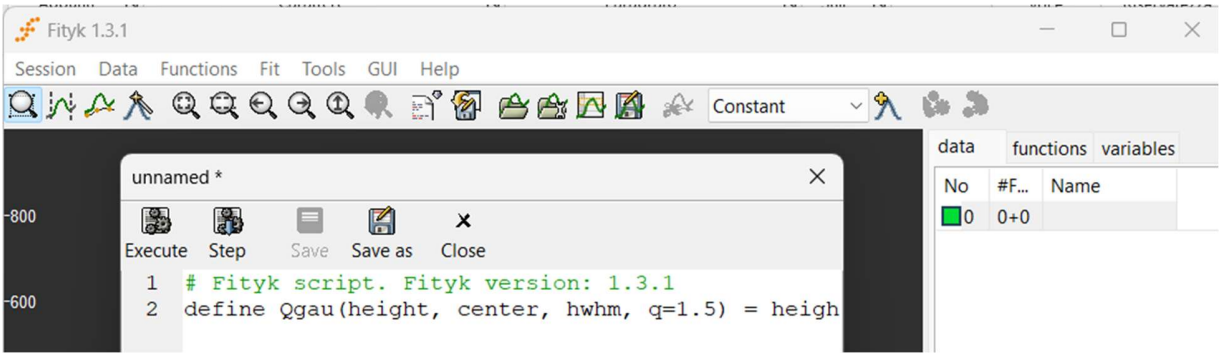

Then, save the Script, and execute it. Using Functions > Definition Manager, in the list of the functions, it will be the q-Gaussian function too.

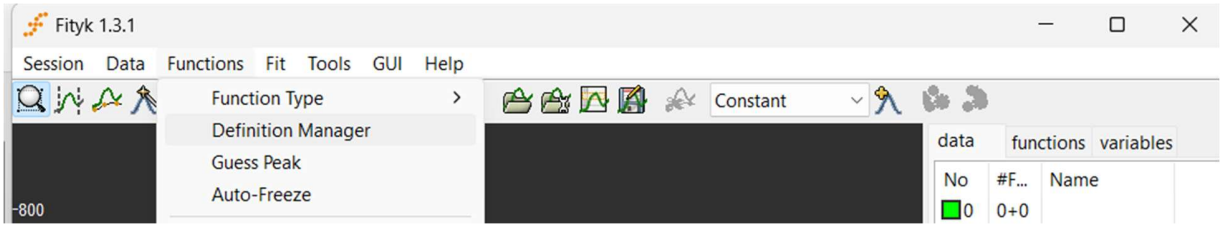

As shown on many occasions, the q-Gaussians are suitable for fitting Raman spectra (by examples proposed in SSRN https://papers.ssrn.com/sol3/papers.cfm?abstract_id=4445044 to the SERS cases, https://chemrxiv.org/engage/chemrxiv/article-details/65092658b6ab98a41cb436e4, for instance). For applying the q-Gaussian functions to the asymmetric bands , https://zenodo.org/records/14220559 , we can define also an asymmetric function, turning the Breit-Wigner-Fano (BWF) function into a q-BWF function (Sparavigna, 2023). Let us write the BWF as follows:

$$\mathrm{BWF}(x) = C\frac{\left[1-\xi\gamma^{1/2}(x-x_o)\right]^2}{[1+\gamma(x-x_o)^2]}$$

When asymmetry parameter ξ is zero, BWF becomes a symmetric Lorentzian function. Note that the center of the line does not correspond to the position of the peak of the function. As in Sparavigna, 2023, https://zenodo.org/records/8356165 , we can define the q-BWF function in the following manner:

$$\text{q-BWF} = C\left[1-\xi\gamma^{1/2}(q-1)^{1/2}(x-x_o)\right]^2[1+(q-1)\gamma(x-x_o)^2]^{1/(1-q)}$$

In fact, the Lorentzian function is substituted by a q-Gaussian function.
In Fityk, the q-Breit-Wigner-Fano (q-BWF)
https://iris.polito.it/retrieve/e7985054-588f-4116-843f-f9d2b5296533/asymm-q.pdf
can be defined as:

Qbreit(height, center, hwhm, q=1.5, xi=0.1) = (1-xi*(q-1)*(x-center)/hwhm)^2 * height*(1+(q-1)^0.5 *((x-center)/hwhm)^2)^(1/(1-q))

And the BWF can be defined as:

Breit(height, center, hwhm, xi=0.1) = (1-xi*(x-center)/hwhm)^2 * height/(1+((x-center)/hwhm)^2)

Using +xi instead of −xi does not change the fitting results in Fityk.

Raman and IR spectra of Paraffin

Raman: Before proposing the ATR-IR fingerprint of paraffin, let us consider its Raman spectroscopy as given by Zheng and Du, 2006. The Raman spectrum of paraffin wax at 20 °C is shown on Fig. 2 by Zheng and Du. "Two dominated groups (3100–2600 and 1500 800 cm^{-1})" are visible. "Most of the assignments of these bands marked in Fig. 2 have been interpreted in the Refs. [17–21]" in Zheng and Du. These references are Edwards and Falk, 1997, Brown et al., 1954, Kalyanasundaram and Thomas, 1976, MacPhail et al., 1984, Meier, 2002). "The strong bands at 2850 and 2890 cm^{-1} are assigned to symmetric and asymmetric CH_2 stretching, respectively. While the symmetric and asymmetric CH_3 stretching cause the two shoulders at 2931 and 2959 cm^{-1}, respectively. A less intense, broad band near 2890 cm^{-1} is attributable to Fermi resonance between CH_2 symmetric stretching and the over tones of the CH_2 bending in the 1440–1460 cm^{-1} region. The band at about 1300 cm^{-1} is due to the CH_2 twisting band. In the C–C stretching region, for an extended chain with all trans structures, there are two intense bands: 1060 and 1130 cm^{-1}, which have been assigned to the symmetric and asymmetric C–C stretching, respectively" (Zheng and Du are mentioning Da Costa et al., 2004).

IR: In https://www.chemicalbook.com/SpectrumEN_8012-95-1_IR1.htm we can find the IR spectrum with peaks given at: 722, 1162, 1304, 1366, 1377, 1462, 2725, 2854, and 2925 cm^{-1}.

In Fig.3 of Khanifah et al., 2018, we can find the "FTIR characteristics of paraffin" at: 719, 729, 889, 1126, 1378, 1463, 1473, 2330, 2634, 2849, 2917, and 2956 cm^{-1}. According to Table 2 by Khanifah and coworkers, we find the assignments:

Wavenumber (cm^{-1})	Mode
2956-2849	(C-H) alkane
2634	(O-H)
1473-1379	(-C-H)
729-719	(CH_2)

In the following part of our work, we provide ATR-IR spectral deconvolutions for paraffin in the form of screenshots of Fityk software, where the green dots are data, red curves the q-BWF components, yellow curve the sum of components. In the lower part of the screenshot, the misfit is given (difference between data and yellow curve).

Data are from the "FTIR spectral library of the major components of archaeological sediments", by Michael Toffolo (Project leader), released under Creative Commons Attribution 4.0 International, available https://zenodo.org/records/14170891 .

Supplementary material is providing the Fityk file. At DOI: 10.5281/zenodo.15167750

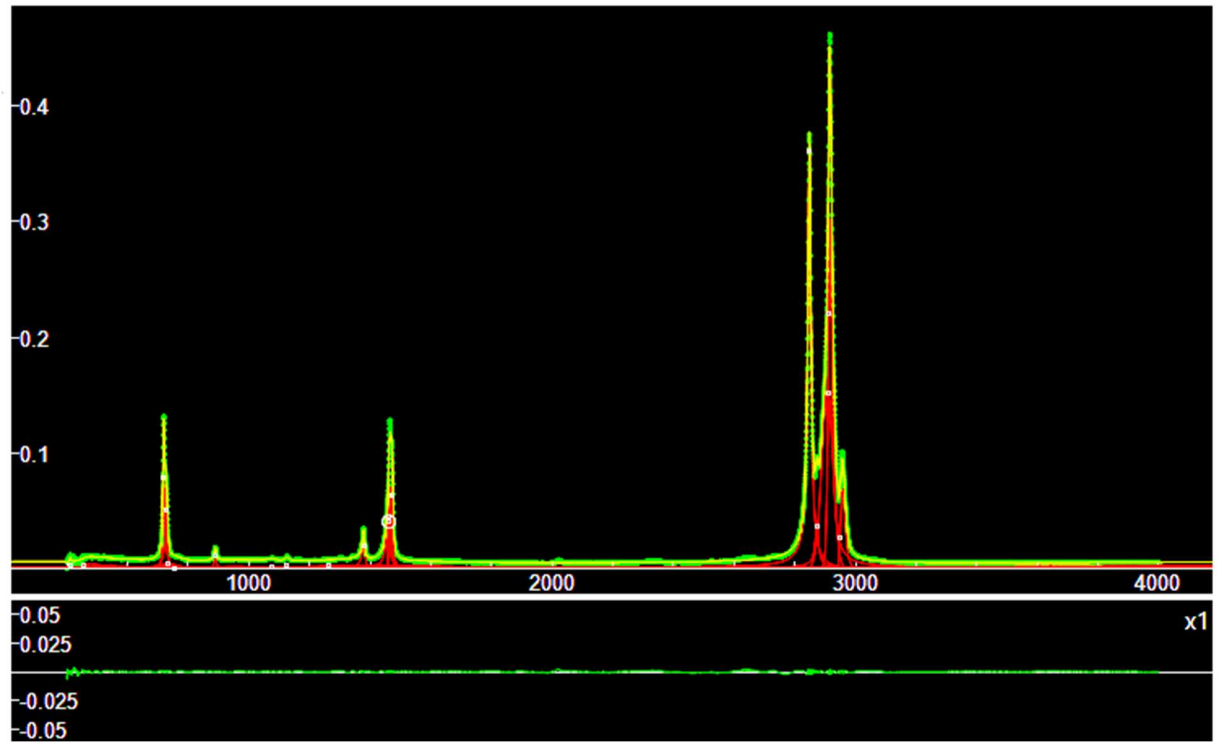

Fig.1: The complete spectrum

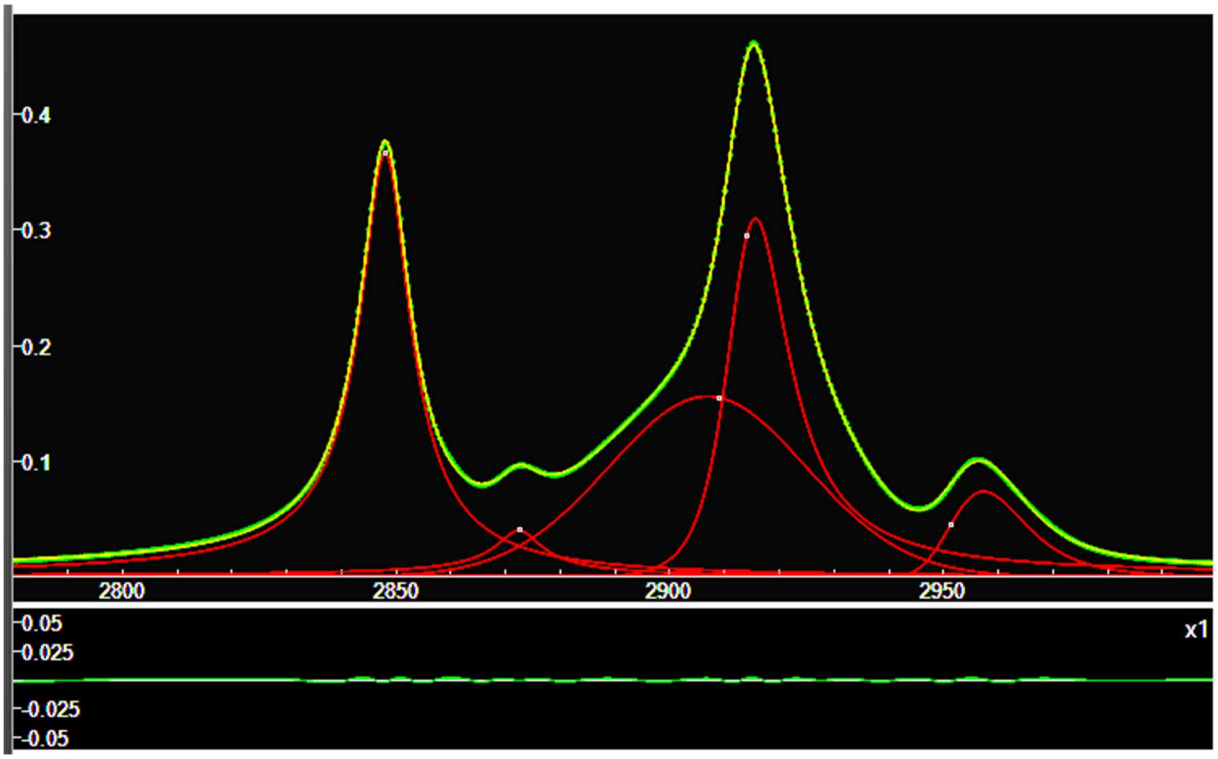

Fig.2: Detail of the deconvolution. Six q-BWF functions are shown.

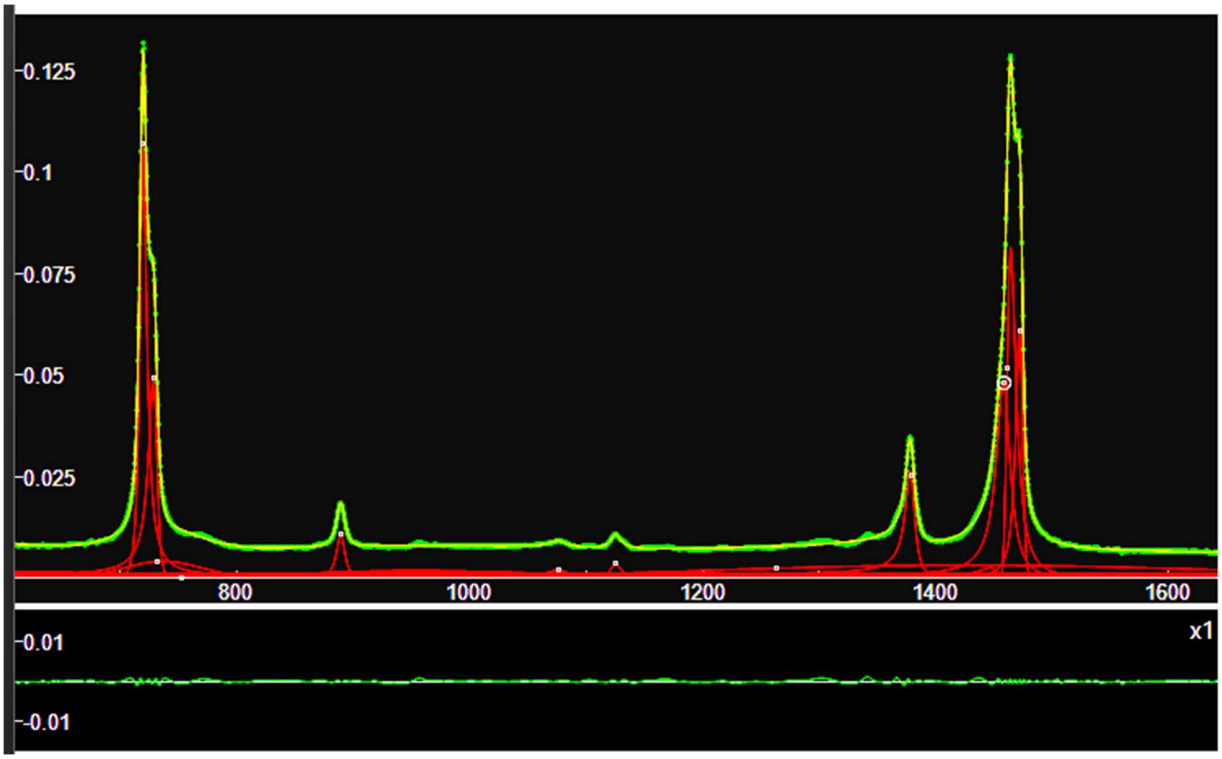

Fig.3: Another part of the spectrum.

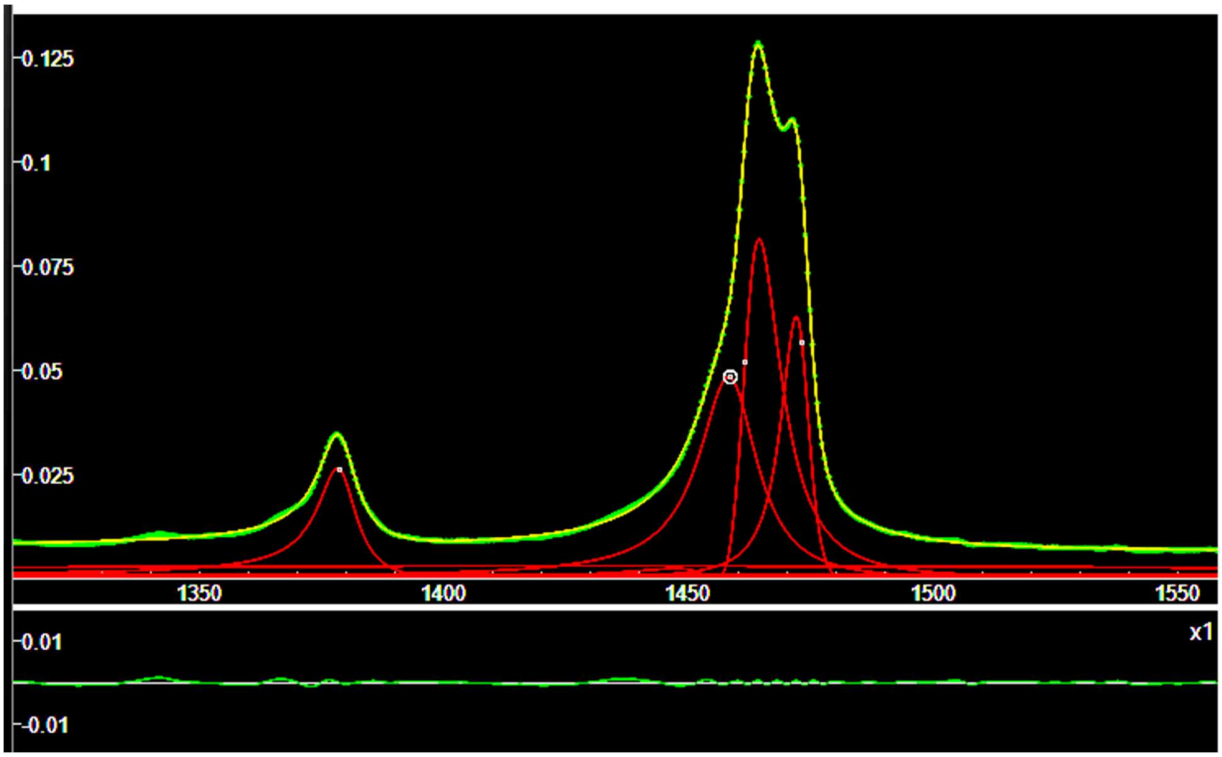

Fig.4: Other details of the deconvolution.

From the figures given above, we can see that the q-BWF functions are asymmetric and then with centers that do not coincide with the peak of the function.
Let us consider the positions of the peaks. They are (in cm^{-1}):

719, 728, 889, 1125, 1378, 1458, 1464, 1472, 2848, 2872.5, 2906, 2916, 2957.

Let us compare these peaks with those given by ChemicalBook:

722, 1162, 1304, 1366, 1377, 1462, 2725, 2854, 2925

and by Khanifah et al., 2018:

719, 729, 889, 1126, 1378, 1463, 1473, 2330, 2634, 2849, 2917, 2956.

We find an excellent agreement in the case of Khanifali and coworkers' data.

References

1. Araki, T., Finney, J. J., & Zoltai, T. (1968). The crystal structure of augelite. American Mineralogist: Journal of Earth and Planetary Materials, 53(7-8), 1096-1103.
2. Brown, J. K., Sheppard, N., & Simpson, D. M. (1954). The interpretation of the infra-red and Raman spectra of the n-paraffins. Philosophical Transactions of the Royal Society of London. Series A, Mathematical and Physical Sciences, 247(922), 35-58.
3. Chatzipanagis, K., Omar, J., & Sanfeliu, A. B. (2024). Assessment of Beeswax Adulteration by Paraffin and Stearic Acid Using ATR-IR Spectroscopy and Multivariate Statistics—An Analytical Method to Detect Fraud. Foods, 13(2), 245.
4. Da Costa, A. A., Marques, M. P. M., & De Carvalho, L. B. (2004). Intra-versus interchain interactions in α, ω-polyamines: a Raman spectroscopy study. Vibrational spectroscopy, 35(1-2), 165-171.
5. Edwards, H. G. M., & Falk, M. J. P. (1997). Fourier-transform Raman spectroscopic study of unsaturated and saturated waxes. Spectrochimica Acta Part A: Molecular and Biomolecular Spectroscopy, 53(14), 2685-2694.
6. Fenske, M. R., Braun, W. G., Wiegand, R. V., Quiggle, D., McCormick, R., & Rank, D. H. (1947). Raman spectra of hydrocarbons. Analytical Chemistry, 19(10), 700-765.
7. Hanel, R., Thurner, S., & Tsallis, C. (2009). Limit distributions of scale-invariant probabilistic models of correlated random variables with the q-Gaussian as an explicit example. The European Physical Journal B, 72(2), 263.
8. Jamwal, R., Kumari, S., Dhaulaniya, A. S., Balan, B., & Singh, D. K. (2020). Application of ATR-FTIR spectroscopy along with regression modelling for the detection of adulteration of virgin coconut oil with paraffin oil. LWT, 118, 108754.
9. Kalyanasundaram, K., & Thomas, J. K. (1976). The conformational state of surfactants in the solid state and in micellar form. A laser-excited Raman scattering study. The Journal of Physical Chemistry, 80(13), 1462-1473.
10. Khanifah, L., Widodo, S., Widarto, W., Putra, N. M. D., & Satrio, A. (2018). Characteristics of paraffin shielding of kartini reactor, Yogyakarta. AJSTD 35, 195–198. doi: 10.29037/ajstd.526
11. MacPhail, R. A., Strauss, H. L., Snyder, R. G., & Elliger, C. A. (1984). Carbon-hydrogen stretching modes and the structure of n-alkyl chains. 2. Long, all-trans chains. The journal of physical chemistry, 88(3), 334-341.

12. Meier, R. J. (2002). Studying the length of trans conformational sequences in polyethylene using Raman spectroscopy: a computational study. Polymer, 43(2), 517-522.
13. Sparavigna, A. C. (2023). SERS Spectral Bands of L-Cysteine, Cysteamine and Homocysteine Fitted by Tsallis q-Gaussian Functions. International Journal of Sciences, 12(09), 14-24.
14. Sparavigna, A. C. (2023). q-Gaussian Tsallis Line Shapes and Raman Spectral Bands. International Journal of Sciences, 12(03), 27-40.
15. Sparavigna, A. C. (2023). q-Gaussian Tsallis Line Shapes for Raman Spectroscopy (June 7, 2023). SSRN Electronic Journal. DOI: 10.2139/ssrn.4445044
16. Sparavigna A. C. (2023). Tsallis q-Gaussian function as fitting lineshape for Graphite Raman bands. ChemRxiv. Cambridge: Cambridge Open Engage; 2023.
17. Sparavigna, A. C. (2023). Asymmetric q-Gaussian functions generalizing the Breit-Wigner-Fano functions. Zenodo. https://doi.org/10.5281/zenodo.8356165
18. Sparavigna, A. C. (2024). Raman and Attenuated Total Reflectance Infrared RRUFF Spectra: some cases of deconvolution with q-Gaussians and q-BWF functions. SSRN Electronic Journal, DOI: 10.2139/ssrn.4993668
19. Sparavigna, A. C. (2024). Atlas of Metabolite SERS Fingerprints obtained by means of q-Gaussian deconvolutions and Fityk Software. ChemRxiv. DOI: 10.26434/chemrxiv-2024-85l19-v2
20. Sparavigna, A. C. (2024). Hydroxyl-Stretching Region in the Raman Broad Scans on Minerals of the Vivianite Group (Vivianite, Baricite, Bobierrite, Annabergite, Erythrite). International Journal of Sciences, 13(08), 23-36.
21. Sparavigna, A. C. (2025). Albite Feldspar Mineral Raman and ATR-IR Fingerprints obtained with q-Gaussian and q-BWF deconvolutions made by means of Fityk Software. Zenodo. https://doi.org/10.5281/zenodo.14743007
22. Sparavigna, A. C. (2025). Augelite Raman and ATR-IR Fingerprints obtained with q-Gaussian and q-BWF deconvolutions made by means of Fityk Software. Zenodo. https://doi.org/10.5281/zenodo.15007192
23. Sparavigna, A. C. (2025). Augelite Raman and ATR-IR spectral deconvolutions in Fityk Software .fit and .peaks files [Data set]. Zenodo. https://doi.org/10.5281/zenodo.15007133
24. Svečnjak, L., Baranović, G., Vinceković, M., Prđun, S., Bubalo, D., & Tlak Gajger, I. (2015). An approach for routine analytical detection of beeswax adulteration using FTIR-ATR spectroscopy. Journal of Apicultural Science, 59(2), 37–49. doi:10.1515/JAS-2015-0018
25. Toffolo, M. (2024). FTIR spectral library of the major components of archaeological sediments [Data set]. Zenodo. https://doi.org/10.5281/zenodo.14170891
26. Tsallis, C. (1988). Possible generalization of Boltzmann-Gibbs statistics. Journal of statistical physics, 52, 479-487.
27. Wojdyr, M. (2010). Fityk: a general-purpose peak fitting program. Journal of applied crystallography, 43(5), 1126-1128.
28. Zheng, M., & Du, W. (2006). Phase behavior, conformations, thermodynamic properties, and molecular motion of multicomponent paraffin waxes: A Raman spectroscopy study. Vibrational Spectroscopy, 40(2), 219-224.